

Short Communication

## Biosynthesis and Characterization of LiFePO<sub>4</sub>/C Composite Using Baker's Yeast

Yue Cao<sup>1,2</sup>, Wangjun Feng<sup>1,2,\*</sup>, Wenxiao Su<sup>2</sup>

<sup>1</sup> State Key Laboratory of Advanced Processing and Recycling Nonferrous Metals, Lanzhou University of Technology, Lanzhou 730050, China

<sup>2</sup> School of Science, Lanzhou University of Technology, Lanzhou 730050, China

\*E-mail: [wjfeng@lut.cn](mailto:wjfeng@lut.cn)

Received: 21 April 2018 / Accepted: 2 June 2018 / Published: 5 July 2018

---

Based on the biosynthesis method, an ellipsoidal LiFePO<sub>4</sub>/C composite is successfully prepared by a simple and effective biomimetic hydrothermal method. Baker's yeast cells not only as structural templates but also as bio-carbon sources in the process of biosynthesis. As a result, the best LiFePO<sub>4</sub>/C composite shows a very high capacity of 158.6mAh g<sup>-1</sup> at 0.1C, which is much higher than pristine LiFePO<sub>4</sub> material (124.7mAh g<sup>-1</sup> at 0.1C). Also, cyclic voltammogram and electrochemical impedance spectra measurement demonstrate that the LiFePO<sub>4</sub>/C composites with Baker's yeast cells have excellent and reversible electrochemical performance. Therefore, biosynthesis would become an effective method for making high-power lithium ion batteries.

---

**Keywords:** LiFePO<sub>4</sub>/C composite, biosynthesis, bio-carbon sources, Baker's yeast cells, electrochemical performance

### 1. INTRODUCTION

For the past few years, amorphous and crystalline materials have been synthesized via biomineralization in biological system[1–3]. Typically, inorganic particles are closely combined with the surface of biological templates by the function of biological adsorption, electrostatic force, hydrogen bond, Van der Waals force, ect. Then, the inorganic particles will nucleate and grow further. Last, it will constitute a new function material that has specific size, morphology and structure with biocomposites. Compared with other traditional methods, the biomineralization processes have markedly advantages, such as molecular control. Crystallographic orientation can be effectively conducted, and materials can be obtained in an environmentally system[4]. Also, the cheap Baker's

yeast cells are used as not only template but also bio-carbon sources, which can prepare the composites with a certain shape and carbon layers.

In view of this, many researchers have prepared advanced mesoporous materials via biosynthesis[5–8]. Rinaldi et al[9] reviewed on the improved of lignin's biosynthesis and structure, differences in structure and chemical bonding between native and technical lignin, and the relationship between lignin structure and catalyst performance, which showed that biosynthesis have a great effect on materials' performance. Chang et al[10] prepared mesoporous  $\text{TiO}_2$  and mesoporous  $\text{Co}_3(\text{PO}_4)_2$ , which had been synthesized by Baker's yeast cells as both bio-templates and carbon source. Du et al[11] synthesized mesoporous  $\text{Li}_3\text{V}_2(\text{PO}_4)_3/\text{C}$  composites by Baker's yeast cells, which exhibited a high discharge rate capacity (126.7 mAh/g at 0.2C) and a large  $\text{Li}^+$  diffusion coefficient. It follows that a new method can be used to synthesize composite materials.

In this work,  $\text{LiFePO}_4/\text{C}$  composites are obtained by a biosynthesis method using Baker's yeast cells as both structural template and bio-carbon source. The material structure, morphology and electrochemical properties for  $\text{LiFePO}_4/\text{C}$  are investigated carefully.

## 2. EXPERIMENTAL SECTION

### 2.1 Material Preparation

The reagents employed in this work are  $\text{FeSO}_4 \cdot 7\text{H}_2\text{O}$ ,  $\text{LiOH} \cdot \text{H}_2\text{O}$ ,  $\text{H}_3\text{PO}_4$ ,  $\text{C}_6\text{H}_8\text{O}_7 \cdot \text{H}_2\text{O}$ , Glucose and Baker's yeast cells. Firstly, quantitative instant dry yeasts (10g/L, 20g/L, and 30g/L) are cultivated in glucose solution at a suitable temperature. Then, stoichiometric amount of  $\text{FeSO}_4 \cdot 7\text{H}_2\text{O}$ ,  $\text{LiOH} \cdot \text{H}_2\text{O}$  and  $\text{H}_3\text{PO}_4$  are dissolved in 50mL distilled water respectively. Then, yeast cells are dumped in the solution of  $\text{FeSO}_4 \cdot 7\text{H}_2\text{O}$  under stirring for 0.5h. After that, the other solutions are dropped into it and stir 0.5h. The mixture is transferred into Teflon-lined stainless steel autoclaves and heat at  $180^\circ\text{C}$  for 6h. After cooling to room temperature, the precursors are washed several times, then drying at  $80^\circ\text{C}$  for 12h. The raw  $\text{LiFePO}_4/\text{C}$  composites are acquired by annealing at  $700^\circ\text{C}$  for 5h in a nitrogen atmosphere with a heating rate of  $5^\circ\text{C}/\text{min}$ .

### 2.2 Characterization

The phase identification of all samples is carried out by powder X-ray diffraction (XRD, Bruker D8, Cu  $\text{K}\alpha$  radiation) from  $10^\circ$  to  $80^\circ$ . The microstructure and morphology of all samples are collected by scanning electron microscope (SEM, JSM-6700F system) operated with accelerating voltage of 20 kV.

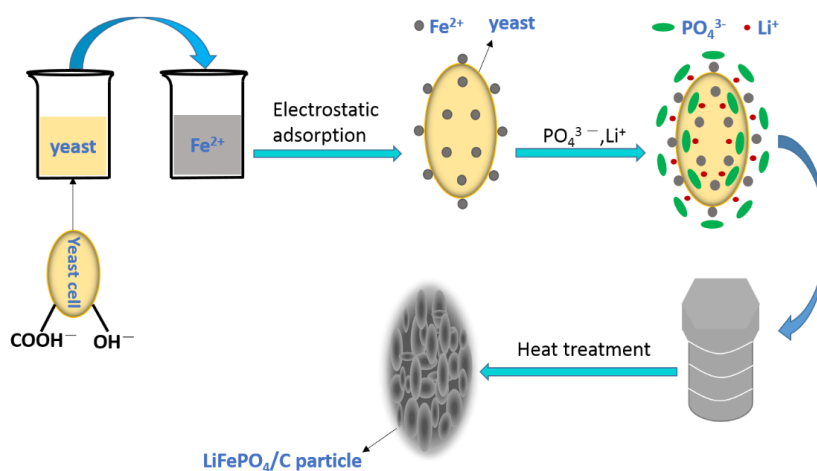
### 2.3 Electrochemical Analysis

Electrochemical performances of the samples are evaluated by CR2025 coin-type cells with lithium metal as the counter electrode. The working electrode is prepared by the mixture of 80wt%

active material, 10wt% acetylene black and 10wt% Polyvinylidene Fluoride (PVDF), which are added in N-methylpyrrolidone (NMP) solvent to form homogeneous slurry. The slurry is coated on an aluminum foil, and dried in a vacuum oven at 120°C for 10h. The cells are assembled in a high-purity argon filling glove box. The Land CT2001A battery test system (Wuhan, China) is used for the charge-discharge tests between 2.4V and 4.3V at room temperature. The electrochemical impedance and cyclic voltammetry measurement are tested on electrochemical workstation. Electrochemical impedance spectra measurement (EIS) is also recorded with the frequency ranging from 100kHz to 10mHz. The voltage range of the cyclic voltammogram (CV) measurements is 2.5-4.2V and the scanning rate is 0.5mV s<sup>-1</sup>.

### 3. RESULTS AND DISCUSSION

Scheme 1 shows the schematic illustration of the synthesis process of LiFePO<sub>4</sub>/C precursor, which the spherical or elliptical yeast cells are used as both structural templates and biocarbon sources[12]. The cell wall of yeast cell is made up of proteins and polysaccharides, which possesses many biomacromolecules and surface charges. They can interact with metal ions or charged ionic groups, provoke the deposition of mineral, provide oriented nucleation sites, immobilize the particles, and finally establish microsphere structure[13,14]. There are hydrophilic anion groups (COOH<sup>-</sup> and OH<sup>-</sup>) on the cell wall surface and inside the yeast cell that can improve the mineralization ability of yeast cells and regulate crystal nucleation and growth[15]. When Fe<sup>2+</sup> were mixed with purified yeast cells, the Fe<sup>2+</sup> cations were combined with the negatively charged groups, and self-assembled to the yeast cell wall surface and cell interior, which is due to electrostatic interaction. Then, Li<sup>+</sup> and PO<sub>4</sub><sup>3-</sup> ions were added into Fe<sup>2+</sup>/yeast solution, respectively, so LiFePO<sub>4</sub>/yeast precursor was formed. Finally, the precursor was processed by heat treatment in stainless steel autoclaves at 180°C for 6h and annealed in a nitrogen atmosphere at 700°C for 5h with a heating rate of 5°C/min, which LiFePO<sub>4</sub>/C particles were obtained. Comparing various materials, it finds that the performance of materials prepared by biosynthesis is better than traditional methods (Table 1.).

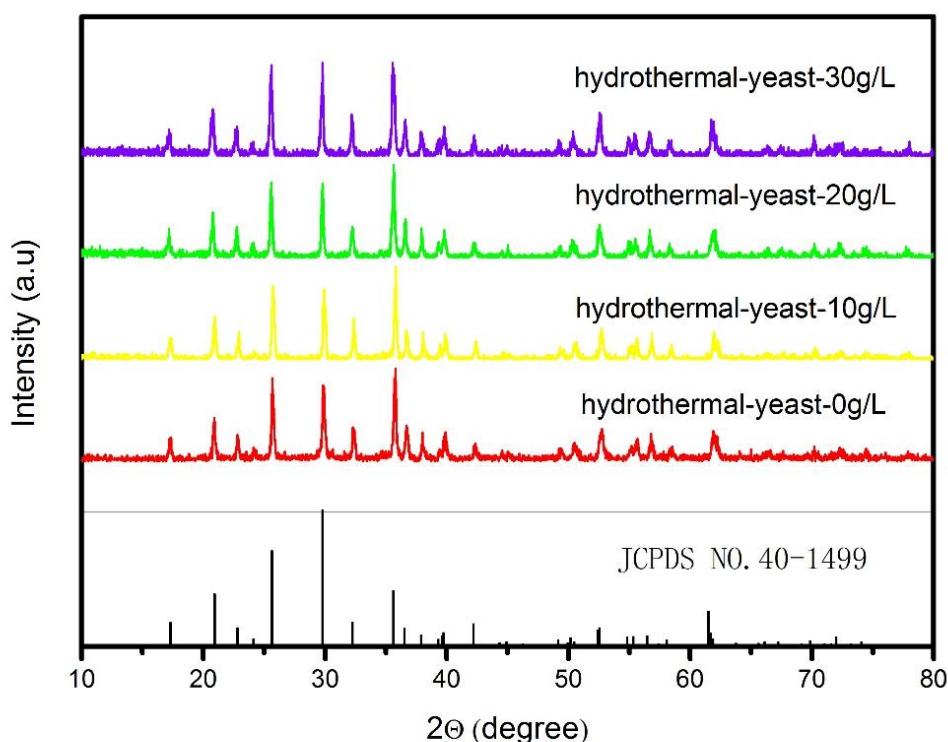


**Scheme 1.** Schematic illustration for the preparation of LiFePO<sub>4</sub>/C composite materials

**Table 1.** Different methods of synthesis there are applied [10-12, 18]

Material	Method	Discharge capacity	Carbon source
TiO <sub>2</sub>	biosynthesis	136mAh g <sup>-1</sup> (at 0.1C)	Baker's yeast cells[10]
Li <sub>3</sub> V <sub>2</sub> (PO <sub>4</sub> ) <sub>3</sub> /C	biosynthesis	126.7mAh g <sup>-1</sup> (at 0.2C)	Baker's yeast cells[11]
LiFePO <sub>4</sub> /C	In-situ synthesis	155mAh g <sup>-1</sup> (at 0.1C)	Glucose[12]
LiFePO <sub>4</sub> /C	hydrothermal method	154.6mAh g <sup>-1</sup> (at 0.1C)	Carbon nanotube[18]

The XRD patterns of all as-prepared composites are shown in Fig.1, the diffraction patterns of the precursors are indexed as orthorhombic olivine-type structure of LiFePO<sub>4</sub> (JCPDS NO.40-1499). It is obviously that main diffraction peaks of all the samples are assigned to the referential diffraction patterns. The peaks of LiFePO<sub>4</sub>/C composites indicate the high purity and no characteristic peaks from carbon and other elements, because the Baker's yeast cells are transformed into amorphous carbon in the process of sintering.

**Figure 1.** XRD patterns of various LiFePO<sub>4</sub> at different additional amount of yeast cells

The morphological features of all as-prepared products are characterized by SEM in Fig.2. Fig.2 (a) shows the SEM image of LiFePO<sub>4</sub> samples which is made by hydrothermal method. It is obviously observed that the samples are mostly blocky and LiFePO<sub>4</sub> grains are aggregated about 1-3μm in diameter. Fig.2 (b) is LiFePO<sub>4</sub>/C composites using 10g L<sup>-1</sup> yeast cells that only partial particles appear spheroidicity. It can be found in Fig.2 (c) (20g L<sup>-1</sup> yeast cells) that there are uniform distribution of granule between the spheroidicities of LiFePO<sub>4</sub>/C. Fig.2 (d) is the image of LiFePO<sub>4</sub>/C composites with 30g L<sup>-1</sup> yeast cells that displays all particles become spheroidicities following the increasing amount of yeast cells. Comparing LiFePO<sub>4</sub> particles (by hydrothermal method) with other LiFePO<sub>4</sub>/C

composites (by biosynthesis method), it shows that biosynthesis method can not only effectively change the precursors structure but also directly provide the bio-carbon which is benefit to increase the electronic conductivity for the potential active material[16,17].

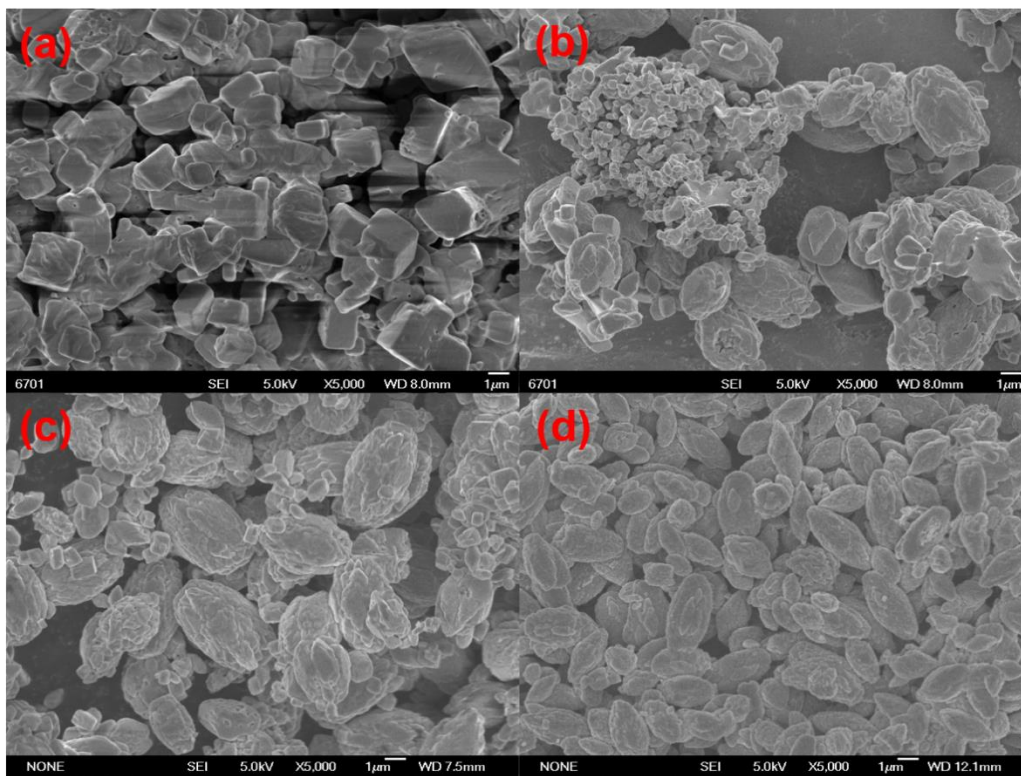


**Figure 2.** SEM images of  $\text{LiFePO}_4/\text{C}$  at different additional amount of yeast cells: (a)  $0\text{g L}^{-1}$ , (b)  $10\text{g L}^{-1}$ , (c)  $20\text{g L}^{-1}$ , (d)  $30\text{g L}^{-1}$

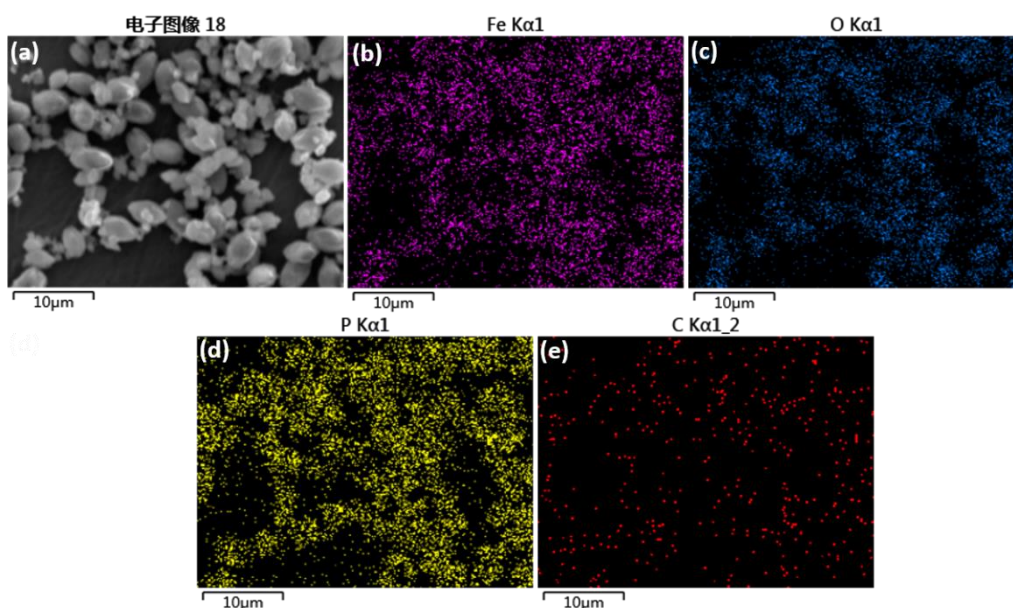


**Figure 3.** SEM image (a) and corresponding EDS mappings (b,c,d,e) of  $\text{LiFePO}_4/\text{C}$  with  $20\text{g L}^{-1}$  yeast cells

For confirming the elements in  $\text{LiFePO}_4/\text{C}$  composites, the elemental distribution mappings of  $\text{LiFePO}_4/\text{C}$  with  $20\text{g L}^{-1}$  yeast cells are characterized in Fig.3. Fig.3 (a) shows a bright field SEM image of  $\text{LiFePO}_4/\text{C}$  with  $20\text{g L}^{-1}$  yeast cells, EDS analysis shows the distribution of Fe, O, P and C of  $\text{LiFePO}_4/\text{C}$  sample with  $20\text{g L}^{-1}$  yeast cells, respectively (Fig.3b-e). It illustrates that the mapping images of Fe, O and P are closely matched with the corresponding SEM image of  $\text{LiFePO}_4/\text{C}$  composites. However, the distribution of C element is not as uniform as Fe, O and P elements, because the content of C is relatively low.

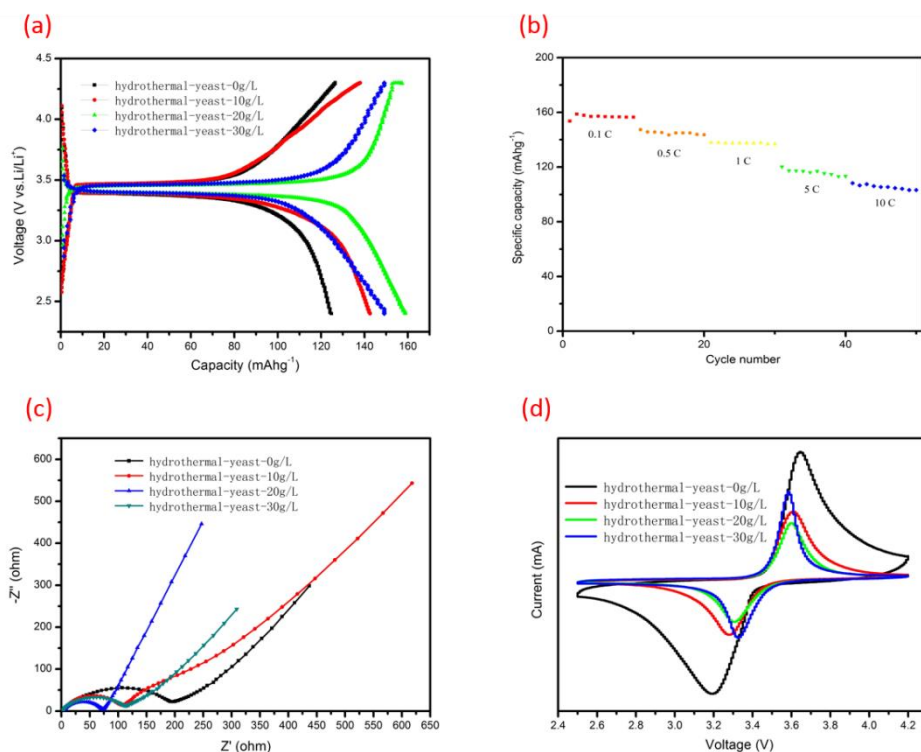


**Figure 4.** (a) Charge/discharge curve of various  $\text{LiFePO}_4/\text{C}$  at 0.1C. (b) Rate performance of  $\text{LiFePO}_4/\text{C}$  with  $20\text{g L}^{-1}$  yeast cells at different current rates. (c) EIS curves of various  $\text{LiFePO}_4/\text{C}$  (d) CV curves of various  $\text{LiFePO}_4/\text{C}$  at a rate of  $0.5\text{mVs}^{-1}$ .

Fig.4. (a) presents the charge/discharge curves of various  $\text{LiFePO}_4/\text{C}$  at 0.1C. The  $\text{LiFePO}_4/\text{C}$  composites using  $20\text{g L}^{-1}$  yeast cells delivers a discharge capacity as high as  $158.6\text{mAh g}^{-1}$ . It is higher than other discharge capacities of  $\text{LiFePO}_4/\text{C}$  cathode materials. The reason could be the homogeneous distribution of granules and spheroidicities, which can effectively shorten the distance and enhance channels for  $\text{Li}^+$  and electron[18]. Comparing the discharge capacity of pure  $\text{LiFePO}_4$  material (by hydrothermal method) with other  $\text{LiFePO}_4/\text{C}$  composites (by biosynthesis method), it demonstrates that the bio-carbon can obviously enhance the discharge capacity. The cycling and rate performance of the sample ( $20\text{g L}^{-1}$  yeast cells) are also investigated at different rates in Fig.4. (b).The specific capacity has any remarkable changes after 10 cycles at different rates, because the particle size and morphology of  $\text{LiFePO}_4/\text{C}$  are benefit for the transmission of  $\text{Li}^+$  and electron[19]. From Fig.4. (c), the impedance spectra curves are composed of a semicircle in the high frequency region and a straight line

in the low frequency region. It shows that the resistance of the LiFePO<sub>4</sub>/C electrode (with yeast cells 20g L<sup>-1</sup>) is much smaller than other samples, which are accord with charge/discharge curves. All CV curves show a pair of well-defined redox peaks in Fig.4. (d), which also corresponds to all above results. In a word, the performance of LiFePO<sub>4</sub>/C composites (by biosynthesis method) are higher than the pure LiFePO<sub>4</sub> material (by hydrothermal method), because the bio-carbon can availably increase the electronic conductivity and enhance channels for electron[20].

#### 4. CONCLUSIONS

In this work, a biosynthesis method is used as a very alternative route to prepare cathode material for lithium ion batteries. The effect of different amount of yeast cells on the characters of LiFePO<sub>4</sub>/C composites is researched roundly. The result demonstrates that the LiFePO<sub>4</sub>/C composites with bio-carbon coating, prepared by biosynthesis method, are more suitable for lithium ion battery. Using biomimetic materials design, high power lithium ion batteries can be prepared by LiFePO<sub>4</sub>/C cathode materials. This important finding has encouraged us to investigate a new biosynthesis method to prepare some composites efficiently.

#### ACKNOWLEDGEMENTS

This work was financially supported by the National Natural Science Foundation of China (No.11264023).

#### References

1. T.M.S. Chang, *Trends Biotechnol.*, 24 (2006) 372.
2. W.A. Hassanain, E.L. Izake, M.S. Schmidt and G.A. Ayoko, *Biosens. Bioelectron.*, 91 (2017) 664.
3. J. Hess, M. Patra, V. Pierroz, B. Spingler, A. Jabbar, S. Ferrari, R.B. Gasser and G. Gasser, *Organometallics*, 35 (2016) 3369.
4. X. Zhang, W. He, Y. Yue, R. Wang, J. Shen, S. Liu, J. Ma, M. Li and F. Xu, *J. Mater. Chem.*, 22 (2012) 19948.
5. T. Fan, B. Sun, J. Gu, D. Zhang and L. W.M. Lau, *Scr. Mater.*, 53 (2005) 893.
6. Y. Xia, W. Zhang, H. Huang, Y. Gan, Z. Xiao, L. Qian and X. Tao, *J. Mater. Chem.*, 21 (2011) 6498.
7. X. Zhang, X. Zhang, W. He, C. Sun, J. Ma, J. Yuan and X. Du, *Colloids Surf. B Biointerfaces*, 103 (2013) 114.
8. Y. Cao, W.J. Feng and W.X. Su, *Int. J. Electrochem. Sci.*, 12 (2017) 9084.
9. R. Rinaldi, R. Jastrzebski, M.T. Clough, J. Ralph, M. Kennema, P.C.A. Bruijninx and B.M. Weckhuysen, *Angew. Chem. Int. Ed.*, 55 (2016) 8164.
10. Y.C. Chang, C.Y. Lee and H.T. Chiu, *ACS Appl. Mater. Interfaces*, 6 (2014) 31.
11. X. Du, W. He, X. Zhang, Y. Yue, H. Liu, X. Zhang, D. Min, X. Ge and Y. Du, *J. Mater. Chem.*, 22 (2012) 5960.
12. H. Gong, H. Xue, T. Wang, J. He, *J. Power Sources*, 318 (2016) 220.
13. W. He, C. Wei, X. Zhang, Y. Wang, Q. Liu, J. Shen, L. Wang and Y. Yue, *Electrochim. Acta*, 219 (2016) 682.

14. E. Nevoigt, *Microbiol. Mol. Biol. Rev.*, 72 (2008) 379.
15. S. Mann, D.D. Archibald, J.M. Didymus, T. Douglas, B.R. Heywood, F.C. Meldrum and N.J. Reeves, *Science*, 261 (1993) 1286.
16. B. Wang, A. Liu, W.A. Abdulla, D. Wang and X.S. Zhao, *Nanoscale*, 7 (2015) 8819.
17. P.L. Kuo, C.H. Hsu, H.T. Chiang and J.M. Hsu, *J. Nanoparticle Res.*, 15 (2013).
18. W.J Feng, Y. Cao, X. Zhao, J.T. Gang and W.X. Su, *Int. J. Electrochem. Sci.*, (2017) 5199.
19. C. Zhang, J. Qi, H. Zhao, H. Hou, B. Deng, S. Tao, X. Su, Z. Wang, B. Qian and W. Chu, *Mater. Lett.*, 201 (2017) 1.
20. R. Muruganatham, M. Sivakumar, R. Subadevi, S. Ramaprabhu and N.L. Wu, *Electron. Mater. Let.*, 11 (2015) 841.

© 2018 The Authors. Published by ESG ([www.electrochemsci.org](http://www.electrochemsci.org)). This article is an open access article distributed under the terms and conditions of the Creative Commons Attribution license (<http://creativecommons.org/licenses/by/4.0/>).